

Accepted Intl. Congr. Catal.
11th, June 1996, Baltimore.

CONF-9606217-- subject to minor revisions.

Nanoscale Attrition During Activation of Precipitated Iron Fischer-Tropsch Catalysts: Implications for Catalyst Design

A. K. Datye^a, M. D. Shroff^a, Y. Jin^a, R. P. Brooks^a, J. A. Wilder^a, M. S. Harrington^b, A. G. Sault^b and N. B. Jackson^b

^aDepartment of Chemical and Nuclear Engineering and UNM/NSF Center for Micro-Engineered Ceramics, University of New Mexico, Albuquerque, NM 87131, USA.

^bProcess Research Department, Sandia National Laboratories, Albuquerque, NM 87185, USA

1. INTRODUCTION

The Fischer-Tropsch Synthesis (FTS) for the production of liquid hydrocarbons from coal-based synthesis gas has been the subject of renewed interest for conversion of coal to liquid fuels. The use of synthesis gas from modern energy-efficient gasifiers requires catalysts that can operate under low H₂/CO ratios, typically 0.7-0.9 (1). Since the FTS stoichiometry requires a H₂/CO ratio of 2.0, catalysts that operate at lower ratios must catalyze the water gas shift reaction to make up the deficit in H₂. The use of iron-based catalysts for the process is attractive in view of their low cost, ready availability and high water-gas shift reactivity. Furthermore, iron catalysts at elevated pressures (10-15 atmospheres) produce the desired range of liquid hydrocarbons. All these features make the use of Fe as an F-T catalyst extremely desirable. Since the reaction is highly exothermic, the preferred reactor type for industrial operation is the slurry bubble column reactor. The catalyst for this reactor is precipitated iron oxide which is spray dried to yield particles with diameter of 30-70 μm. One major limitation of these catalysts is that they tend to undergo attrition during use, leading to problems in catalyst separation and recovery of liquid products from the reactor (1).

Our earlier work (2,3) with precipitated iron Fischer-Tropsch catalysts has shown that catalyst attrition occurs at two length scales. First, there is micron-scale attrition that is caused by the weak mechanical binding between the primary particles that make up the precipitated F-T catalyst. This is shown schematically in Fig. 1. There is also a nano-scale attrition which occurs during activation of the F-T catalyst, and is shown schematically in Fig. 2. The catalyst as-prepared, consists of single crystals of hematite (α-Fe₂O₃). Reduction in CO or syngas slowly transforms the catalyst into the carbide phase. The decrease in specific volume going from the hematite to carbide causes a breakup of the original crystals. Carbon deposited during reaction causes these crystallites to be pried apart, and leads to further breakdown of the catalyst.

The work reported in this paper is directed at the development of high activity attrition resistant iron catalysts. Commercial catalysts use binders to improve the attrition resistance of iron catalysts. As we show in this paper, binders such as kaolin which are commonly used in commercial catalysts may not be effective in improving attrition resistance. Other binders, such as silica, which may potentially be effective at improving attrition resistance have been reported to cause a loss of catalyst activity (4). Since the mechanisms by which the oxide binder influences catalyst activity are not well understood, in this study we use model Fe catalysts that allow study of the silica-Fe interface. Finally, the role of Cu on the reducibility of the Fe catalysts has also been studied. Taken together, this work provides the supporting data that will help in the rational design of precipitated Fe catalysts.

RECEIVED
USDOE/PETC

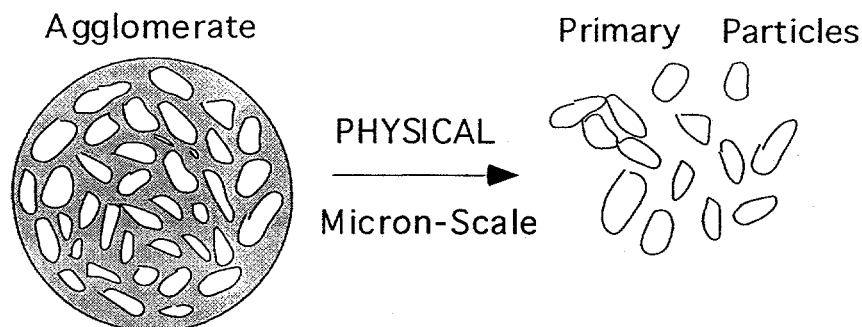


Fig. 1: Schematic illustration of physical or micron-scale attrition where the catalyst agglomerates break down into the primary particles

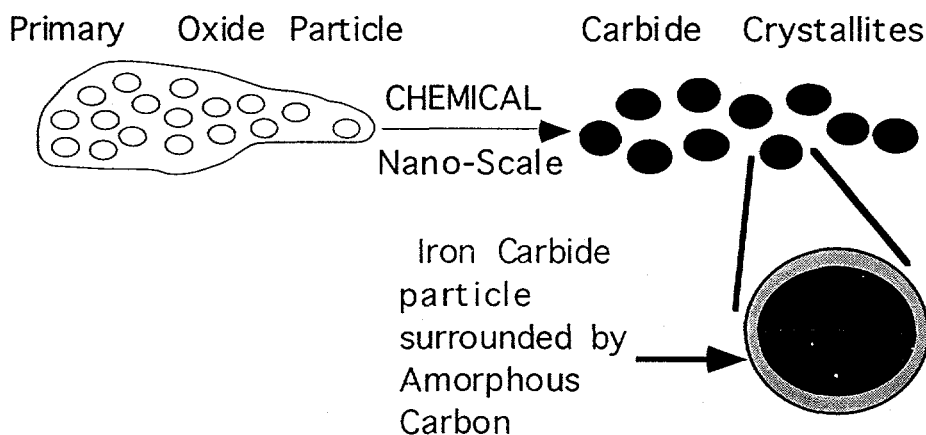


Fig. 2: Schematic illustration of chemical or nano-scale attrition where the primary particles break down into the carbide crystallites

2. EXPERIMENTAL

The commercial catalysts used in this study were prepared by United Catalysts, Inc. for the Department of Energy by precipitation and spray drying. The nominal composition was 88.95% Fe_2O_3 , 11% CuO and 0.05% K_2O for the binderless catalyst and 0.92% K_2O , 5.3% CuO , 63.7% Fe_2O_3 , 30.1% kaolin for the catalyst with binder. In a typical experiment, 1 g of catalyst was treated in a fixed bed flow reactor under various activation and reaction conditions. The activation conditions involved catalyst reduction at atmospheric pressure in H_2 , CO or a 0.7:1 H_2/CO syngas mixture. The catalysts were carefully passivated and then removed from the reactor for analysis by a number of analytical techniques. Details of the analytical equipment and the reactor configuration are described elsewhere (2).

We measured the strength of the catalyst agglomerates using the approach developed by Thoma et al. (5). This involved measuring the particle size distribution before and after applying energy via a calibrated ultrasonic probe. As described by Thoma et al. (5), the ultrasonic energy required to break agglomerates can be related to the agglomerate strength measured by conventional methods such as uniaxial compaction. A Micromeritics Sedigraph 5100 particle size analyzer was used for these experiments.

The effect of copper on iron F-T catalysts was studied by synthesizing a series of samples with Cu/Fe ratios of 0 to 0.25. These samples were reduced in flowing H_2 in the TGA and studied before and after reduction by TEM.

To study the details of the iron-silica interaction, two types of catalysts were prepared. The first, referred to as the model catalyst, was prepared by controlled precipitation of $\text{Fe}(\text{OH})_3$

from a $\text{Fe}(\text{NO}_3)_3$ solution onto 270 nm non-porous Stöber SiO_2 spheres. The nominal Fe loading was 20 wt%. The second, referred to as the co-precipitated catalyst, was prepared by mixing the $\text{Fe}(\text{NO}_3)_3$ and TEOS in ethanol and adding NH_4OH and water to cause the iron and silica to co-precipitate. These samples were studied by XPS, TEM and TGA to determine the reducibility of the iron.

3. RESULTS

3.1 Attrition resistance of commercial catalysts

The Sedigraph particle size distributions on the commercial catalyst containing the kaolin binder are shown in Fig. 3. The catalyst was found to be extremely weak, with particle breakup being initiated by mere recirculation of the slurry. When a ultrasonic energy equivalent to a 200 psi breaking strength was applied, the particles broke down completely to the constituent primary particles. This particle breakup is shown in Fig. 4 where SEM images of the binder-containing catalyst as-received (Fig. 4a) and after ultrasound treatment (Fig. 4b) are compared. Fig. 4a shows a spherical agglomerates 50 μm in diameter while Fig. 4b at the same magnification, shows complete breakup. A similar particle breakup was observed for a binderless catalyst and has been reported by us elsewhere (3). A detailed microscopic study of the binder-containing catalyst revealed severe inhomogeneities in the composition of the catalyst with the binder and the iron oxide appearing as separate phases. Fig. 5 shows a TEM image of the catalyst where the iron oxide and binder phases are clearly seen to be separate and distinct. The addition of binder in the form shown in Fig. 5 does not seem to impart any attrition resistance, and such catalysts would likely break-up during actual use.

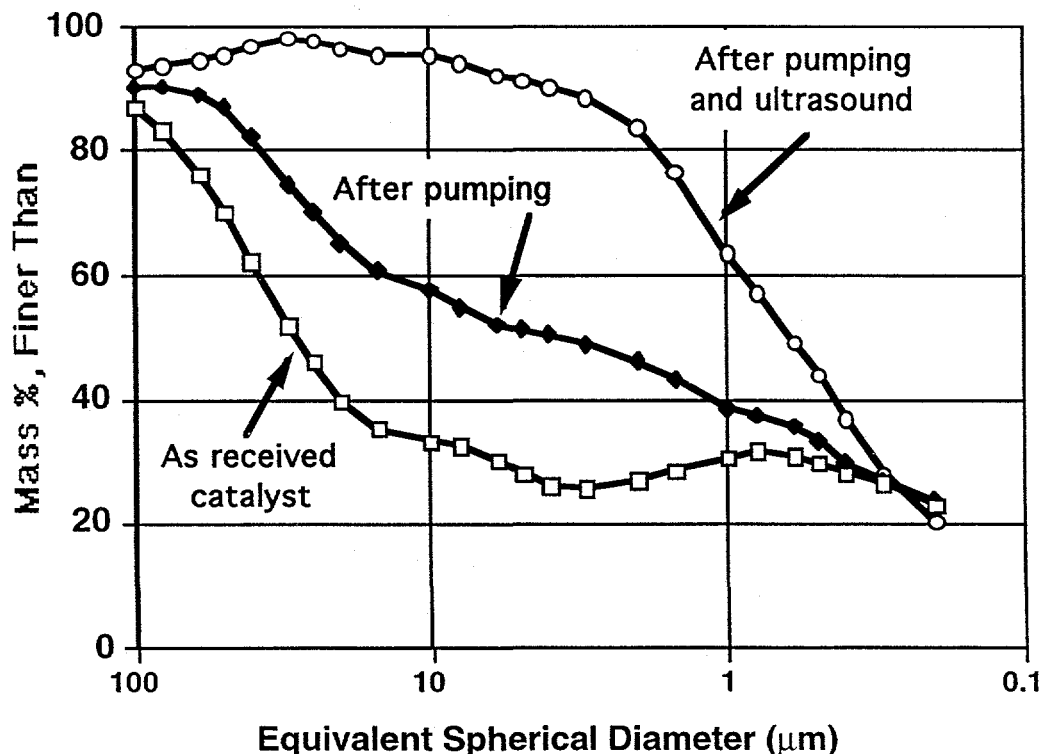


Fig. 3: Sedigraph Particle Size Distributions of the commercial catalyst with a kaolin binder. The catalyst can be seen to break down readily, indicating weak agglomerates.

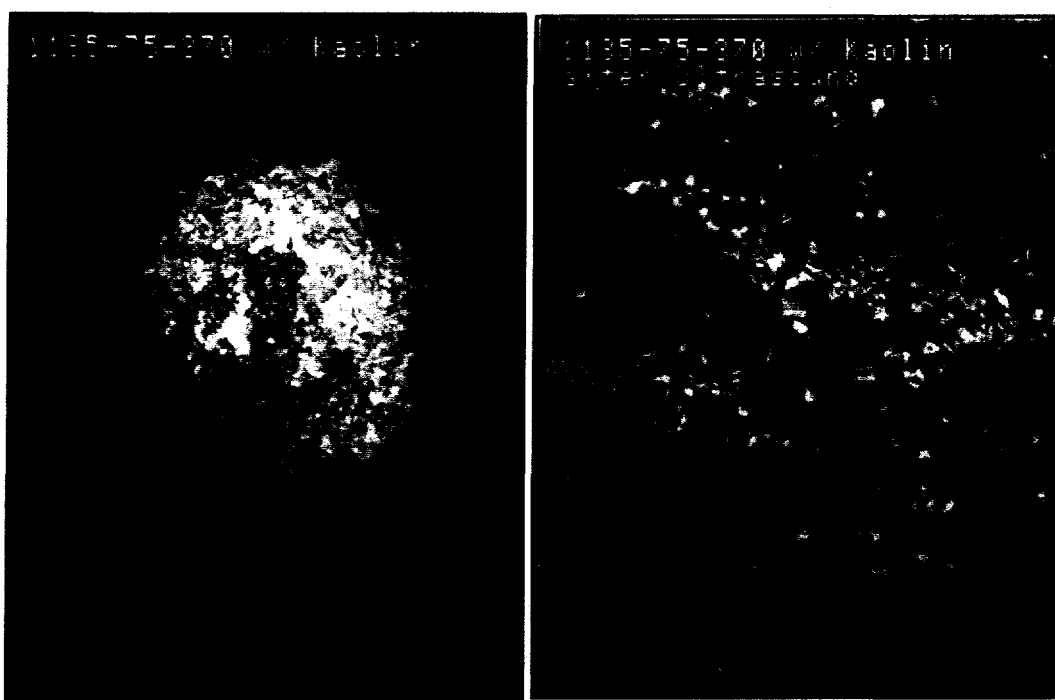


Fig. 4: Scanning electron micrograph of the catalyst with kaolin binder (a) as received and (b) after ultrasonication showing complete breakdown of the spherical agglomerates.

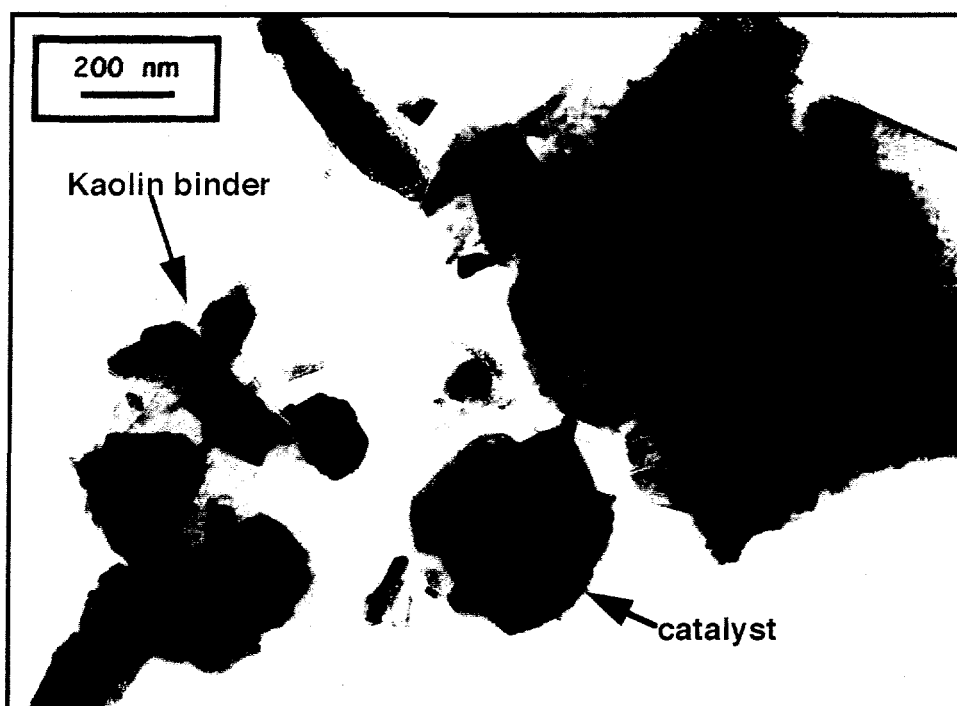


Fig. 5: Transmission electron micrograph of the catalyst with kaolin binder. The binder contains sheets of kaolin.

3.2 Iron/Silica interactions

The inability of the Kaolin binder to improve attrition resistance suggest that other binders should be considered for this catalyst system. While silica is a suitable support and is used in the case of supported cobalt catalysts, addition of silica lowers the catalyst activity of precipitated Fe catalysts (4). It has been suggested that the lower activity comes from the inability to reduce the iron and the formation of iron silicate phases. In order to study these Fe-SiO₂ interactions in greater detail, we have prepared model catalysts where the Fe was supported on non-porous 270 nm Stöber silica spheres. A second type of Fe/SiO₂ catalyst was prepared by co-precipitation of the iron and silica precursors. We studied the ability of these catalysts to undergo reduction and carburization by XPS, TGA and TEM.

The co-precipitated catalyst was examined by XPS before and after reduction in 630 Torr H₂ for 3h at 673K and the results are reported in Fig. 6. The reduction was performed in a reaction chamber that is attached to the XPS analyzer which permits sample transfer without exposure of the samples to ambient air. The as-prepared sample (Fig. 6 curve a) shows a complete absence of any shakeup features between 714 and 720 eV indicating a mixture of Fe⁺² and Fe⁺³. However, the binding energy is substantially higher than expected for a pure iron oxide phase (6) providing a strong indication that an iron silicate is present. After heating in H₂, the peak has shifted to a lower binding energy and a strong shakeup feature is observed at ≈716 eV. The peak shape is typical of a pure Fe⁺² phase, but as in spectrum a) the binding energy is much higher than expected for Fe_xO (6). Hence this spectrum is assigned to a silicate phase containing Fe⁺². The silicate phase is difficult to reduce, as shown by the complete absence of any metallic iron following the reduction. The TGA results of heating this sample in He, CO or H₂ atmosphere showed no effect of the gas atmosphere on the weight change. In all cases, a weight decrease of 25% was seen and is presumably caused by the loss of adsorbed solvent ethanol, and loss of water which would result from the dehydration and condensation reactions. The TEM image of this sample as-prepared is shown in Fig. 7. The sample morphology is unchanged after 723 K reduction in CO or H₂. Electron diffraction shows that this phase is amorphous while Fe and Si peaks can be detected by EDS confirming the co-existence of these two elements. From these results we conclude that co-precipitation leads to a strong interaction between the Fe and SiO₂ forming a glassy phase that renders the Fe unreducible up to 723K.

In contrast to the results on the co-precipitated catalyst, a significant fraction of the Fe in the model catalyst could be reduced in H₂ and then carburized in CO. Fig. 8 shows the XPS spectra of this catalyst as a function of pretreatment. Curve a) shows the as-received catalyst whose features suggest the presence of Fe⁺² and Fe⁺³ and a binding energy (710.2 eV) typical of Fe₂O₃. Heating the sample in 630 Torr H₂ at 673K for 3h yielded the spectrum shown in curve b). A similar spectrum was obtained after 1 h in H₂. The spectrum shows a well resolved metallic Fe peak (706.5 eV) and a shoulder at the position expected for Fe⁺². Background subtraction and peak fitting indicate that ≈30-40% of the detected Fe is metallic. When this sample was further heated to 543 K in 400 Torr CO for 2h, spectrum c) was obtained. The Fe 2p_{3/2} peak shifts by ≈ 0.3 eV to higher binding energy (see figure inset) and a broadening of the C1s peak occurs to low binding energies. Both of these observations are consistent with the formation of iron carbide (6). In order to confirm the small Fe 2p_{3/2} binding energy shift, the peak energy was measured 5-6 times for both the hydrogen reduced and CO treated samples, and the results averaged.

The XPS results are consistent with those of TGA in H₂ which shows a weight decrease of 2% upon heating in H₂. The nominal weight loading for this catalyst was 20 wt% Fe/SiO₂, which would mean that a transformation from Fe₂O₃ --> α-Fe would result in ≈ 8% decrease in weight. This suggests that approximately 25% of the iron in this sample has been reduced. Treatment in CO following the H₂ reduction causes a slow weight gain which is consistent with carbon deposition or carburizing of the sample. The small weight gain does not allow us to estimate the degree of carburizing of the Fe in this sample. Figure 9 shows a TEM image of the sample reduced in H₂ in the TGA and then exposed to CO at 723 K. This catalyst shows two

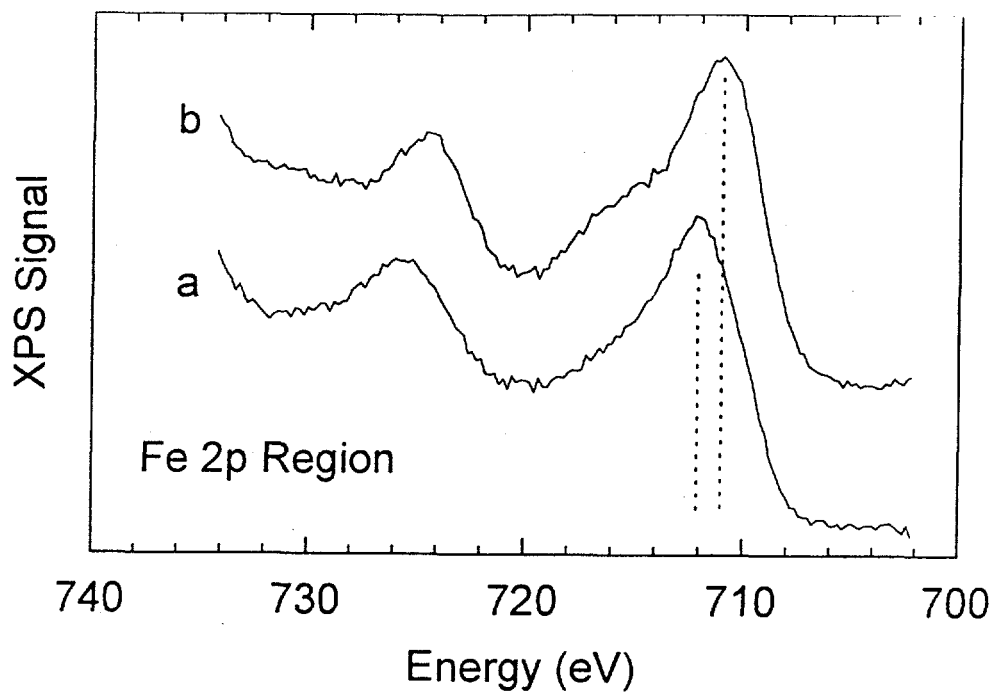


Fig. 6: X-ray photoelectron spectrum of co-precipitated catalyst (a) as prepared and (b) after 3 h of H₂ reduction at 673 K.

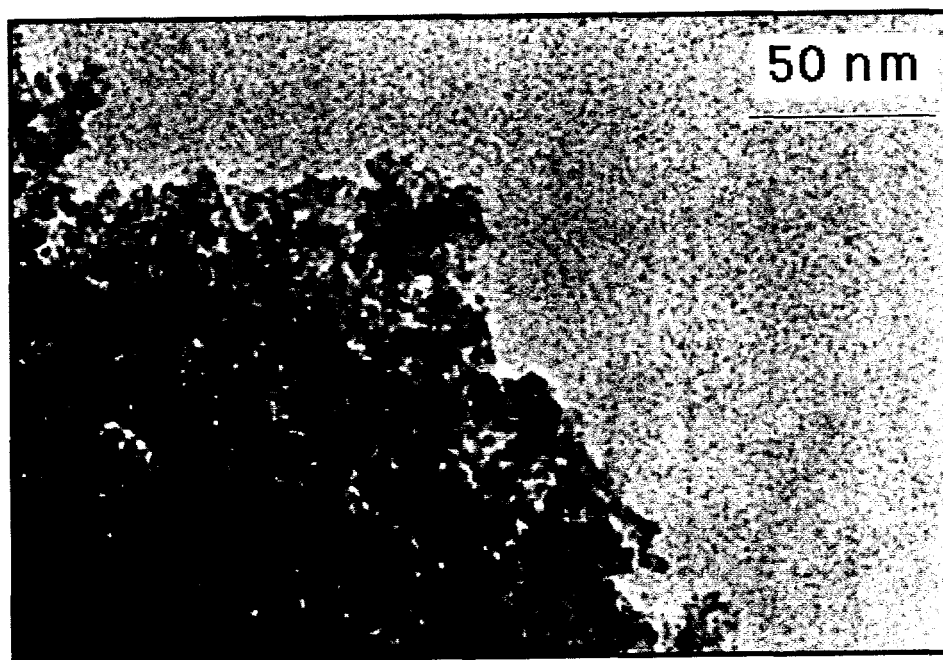


Fig. 7: Transmission electron micrograph of co-precipitated catalyst as-prepared. The sample looks very similar after H₂ reduction and stays amorphous.

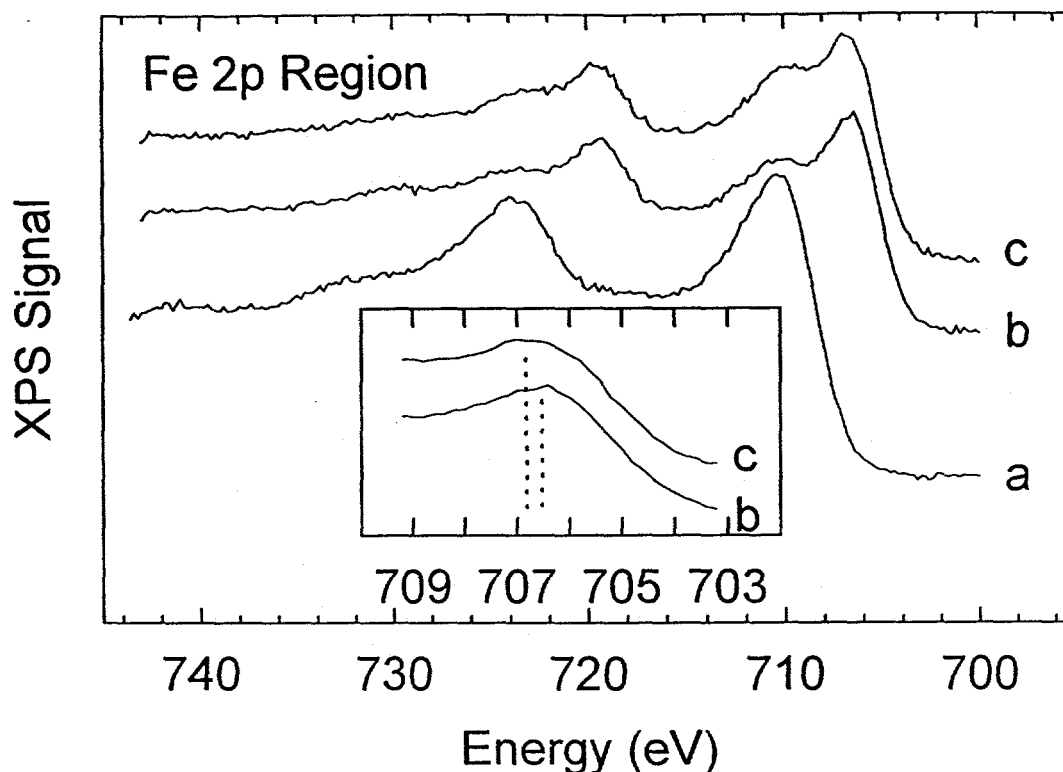


Fig. 8: X-ray photoelectron spectrum of model Fe/SiO₂ catalyst (a) as prepared (b) after H₂ reduction at 723K and c) after 543 K CO treatment following H₂ reduction.

types of Fe particles clearly visible. One of them will be termed the 'cherry-like' structure and is imaged at high magnification in Fig. 9b. These cherry-like particles consist of a core exhibiting 2Å lattice fringes and a skin which is typically amorphous upon initial examination. However, as the particle is exposed to the electron beam, the surface layer crystallizes and shows lattice fringes consistent with magnetite. The 2 Å lattice fringes could arise from α -Fe or from Fe carbide. Based on the fringe spacing alone, we cannot identify which of these phases is present. However, from previous work (2,3) we would expect that the 723 K treatment would definitely carburize the α -Fe to form the carbide. Both CHN elemental analysis as well as H₂ TPR can help determine the identity of the Fe phase and the nature of the carbon deposits in this catalyst. These analyses are presently being performed in our laboratory.

The cherry-like structure consisting of a core of reduced iron and surface magnetite arises due to sample oxidation during passivation of the sample before it is removed from the reactor. We conclude that all particles exhibiting the cherry-like structure represent the reducible iron phase. The extent and thickness of this layer is consistent with that seen in our previous work after careful passivation (7). We have found that if passivation is not performed carefully, the particle may completely transform into magnetite and the core of α -Fe or carbide would not be seen. When catalysts that have been used in F-T synthesis are examined, they contain a surface layer of amorphous carbonaceous material that helps protect the iron carbide phase contained within. However, the sample imaged here had not been used for F-T synthesis and hence did not have the protective carbonaceous layer.

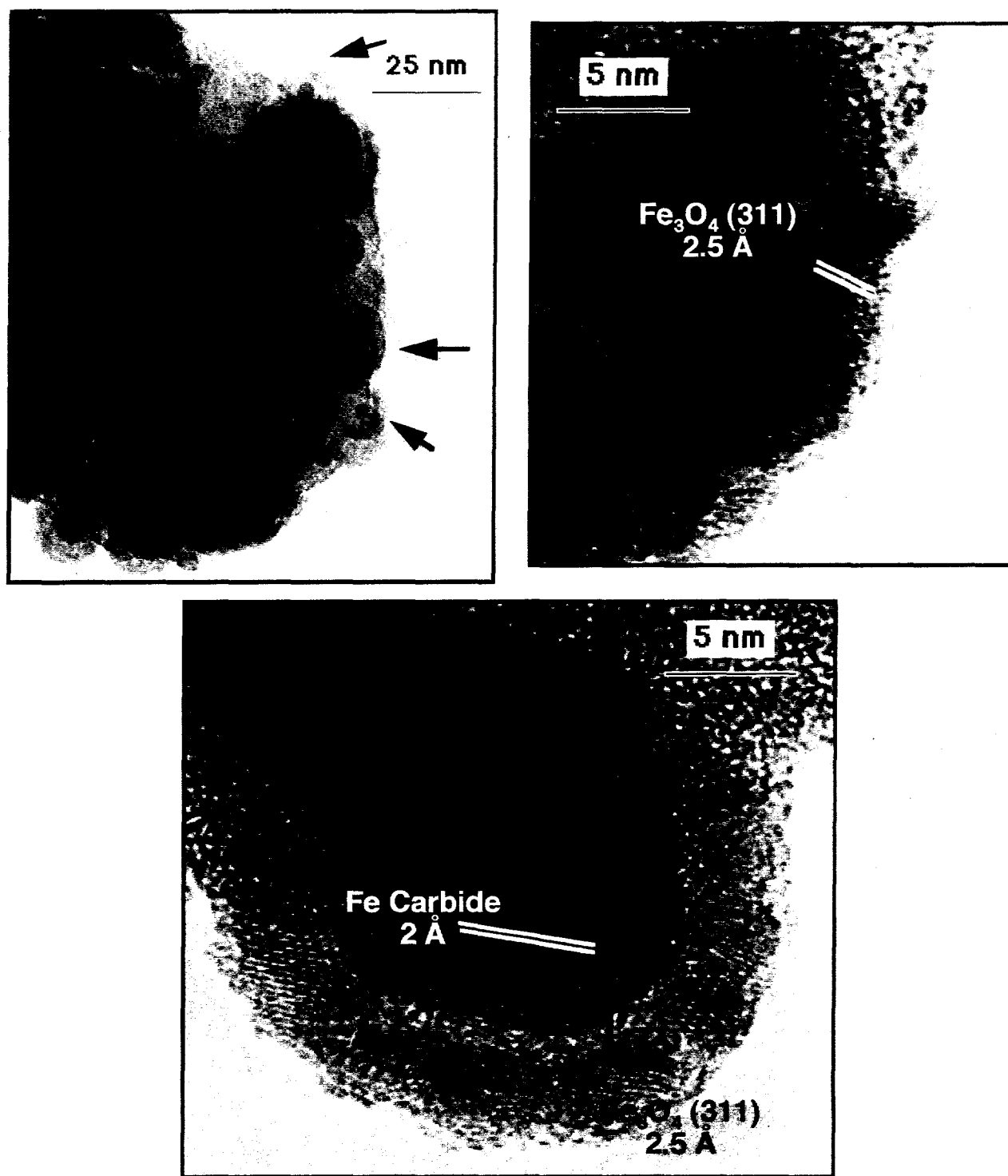


Fig. 9: (a) Transmission electron micrographs of model Fe/SiO₂ catalyst after H₂ and CO treatment in the TGA at 723 K. (b) High magnification view of one of the cherry-like particles seen in Fig. 9(a). (c) High magnification view of the dispersed iron phase showing lattice fringes consistent with magnetite.

In addition to the cherry-like particles, the model catalyst also contained crystalline iron in dispersed form as shown in Fig. 9c. The dispersed iron in all instances showed lattice fringes consistent with magnetite. Since these particles are small, often of the thickness of the passivation layer, it is possible that the passivation process consumed all of the reducible iron present in these small particles. The other possibility is that these dispersed iron particles are more difficult to reduce and represent the unreducible iron seen by XPS (which was identified as magnetite based on the shake-up features). At this stage, we have not determined the reasons why this magnetite phase does not reduce under our conditions, and this is the subject of ongoing work. We have not been able to locate any crystalline phases in addition to magnetite and the iron carbide (or α -Fe depending on whether the catalyst was reduced in CO or H₂). If iron silicate is present, it is probably an amorphous phase (as seen with the co-precipitated catalyst) and therefore difficult to distinguish from the silica support.

3.3 Effect of copper

The effect of addition of copper on the reducibility of iron oxide was studied by preparing a series of samples with Cu/Fe ratios ranging from 0 to 0.25. The TGA profiles for the samples in flowing H₂ are shown in Fig. 10. It is clear that addition of Cu decreases the time for reduction of the iron oxide to metal. However, not all of this copper is incorporated in the metallic Fe. In our previous work on the 11 wt% CuO catalyst, we found that the copper segregated into metallic particles distinct from the reduced iron. If the iron particles during reaction undergo transformation from the carbide to the oxide reversibly, we might expect that the segregated Cu phase may not be beneficial except for the initial reduction. Furthermore, the influence of copper on ease of carburizing the iron has not yet been explored and is presently being studied in our laboratory.

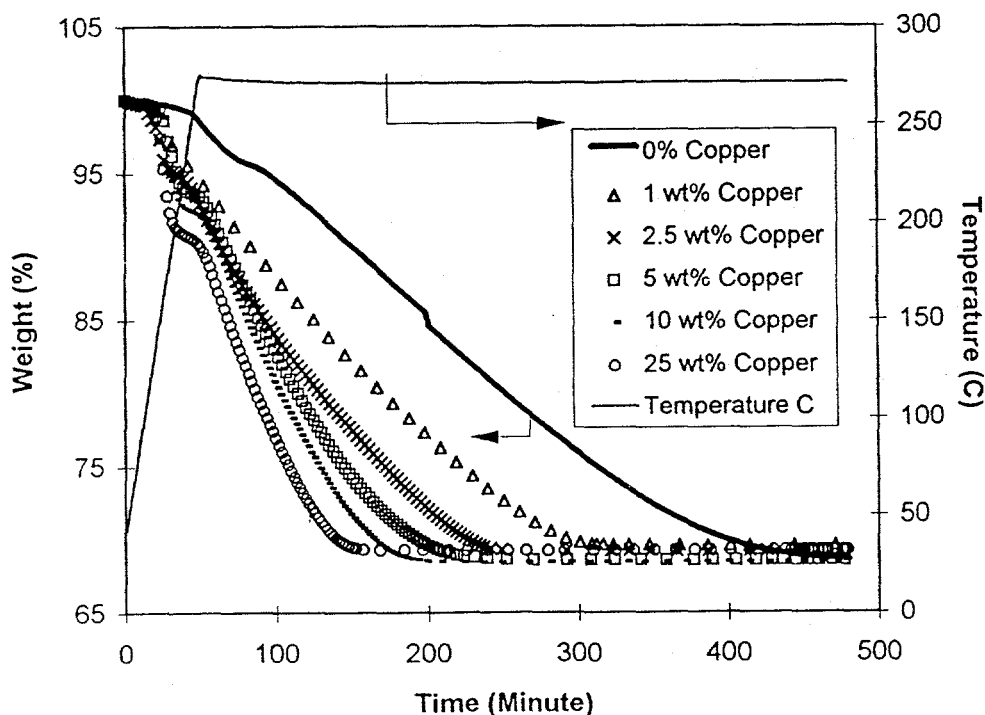


Fig. 10: Reduction of iron samples containing various amounts of copper, as seen in a thermogravimetric analyzer.

4. Summary and Conclusions

This work has shown that the kaolin binder that has been used in commercial F-T catalysts does not offer any significant attrition resistance. This is due in part to its morphology (plate-like) and to its particle size being much greater than the primary crystallite size of the iron oxide catalyst. From a microscopic examination of these catalysts, it appears that if the nanoscale attrition of the iron catalyst is to be avoided, the iron must be well dispersed on the binder, and the binder must provide an interlocking microstructure that provides strength and stability to the 30-70 μm agglomerates.

The study of Fe/SiO₂ catalysts has shown that co-precipitation of the iron and silica leads to formation of an amorphous glassy phase which is difficult to reduce even at 723K. On the other hand, when the iron was precipitated on a preformed silica, 25-40% of the iron could be reduced and carbided. The supported iron catalyst, after reduction, formed 15-20 nm iron carbide particles that look very similar to those on the unsupported catalyst. The major difference is these nanometer sized particles are anchored on a support and therefore would not be expected to breakup further and contribute to the fines generated as catalyst attrition proceeds. However, since only a fraction of the silica-supported iron can be reduced to the active carbide phase, our present efforts are devoted to moderating the Fe/SiO₂ interaction by introducing an interfacial oxide phase. We are also studying the role of added Cu on the ease of reducibility of Fe/SiO₂. The implication of this work is that other binder materials should be explored that have a morphology that can strengthen the agglomerates and minimize the Fe-SiO₂ interfacial reactions. This work is presently underway in our laboratory.

Acknowledgments

This work was supported by the U.S. Department of Energy -contract DE-FG22-95PC95210. The portion of the work performed at Sandia National Laboratories is supported by the US DOE contact DE-AC04-94AL85000. Transmission Electron Microscopy was performed at the Microbeam Analysis Facility within the Department of Earth and Planetary Sciences at the University of New Mexico.

References

- (1) R. D. Srivastava, V. U. S. Rao, G. Cinquegrane, and G. J. Stiegel, *Hydrocarbon Processing*, pg 59, Feb 1990.
- (2) M. D. Shroff, D. S. Kalakkad, K. E. Coulter, S. D. Kohler, M. S. Harrington, N. B. Jackson, A. G. Sault and A. K. Datye, *J. Catal.*, 156, 185 (1995).
- (3) D. S. Kalakkad, M. D. Shroff, S. D. Kohler, N. B. Jackson, A. G. Sault and A. K. Datye, *Appl. Catal.*, in press.
- (4) D. B. Bukur, X. Lang, D. Mukesh, W. Zimmerman, M. Rosynek and C. Li, *Ind. Eng. Chem. Res.* 29, 1588 (1990).
- (5) S. G. Thoma, M. Ciftcioglu and D. M. Smith, *Powder Technology*, 68, 53 (1991).
- (6) C. S. Kuivila, J. B. Butt and P. C. Stair, *Appl. Surf. Sci.*, 32, 99 (1988).
- (7) M. D. Shroff and A. K. Datye, *Catal. Lett.*, in press.

DISCLAIMER

This report was prepared as an account of work sponsored by an agency of the United States Government. Neither the United States Government nor any agency thereof, nor any of their employees, makes any warranty, express or implied, or assumes any legal liability or responsibility for the accuracy, completeness, or usefulness of any information, apparatus, product, or process disclosed, or represents that its use would not infringe privately owned rights. Reference herein to any specific commercial product, process, or service by trade name, trademark, manufacturer, or otherwise does not necessarily constitute or imply its endorsement, recommendation, or favoring by the United States Government or any agency thereof. The views and opinions of authors expressed herein do not necessarily state or reflect those of the United States Government or any agency thereof.

DISCLAIMER

This report was prepared as an account of work sponsored by an agency of the United States Government. Neither the United States Government nor any agency thereof, nor any of their employees, makes any warranty, express or implied, or assumes any legal liability or responsibility for the accuracy, completeness, or usefulness of any information, apparatus, product, or process disclosed, or represents that its use would not infringe privately owned rights. Reference herein to any specific commercial product, process, or service by trade name, trademark, manufacturer, or otherwise does not necessarily constitute or imply its endorsement, recommendation, or favoring by the United States Government or any agency thereof. The views and opinions of authors expressed herein do not necessarily state or reflect those of the United States Government or any agency thereof.